EasyChair Preprint

№ 5062

Finite Element based Natural Frequency Analysis of a Porous Functionally Graded Jeffcott Rotor System subjected to Thermal Gradients

Yash Jaiman and Prabhakar Sathujoda

February 27, 2021

Finite Element based Natural Frequency Analysis of a Porous Functionally Graded Jeffcott Rotor System subjected to Thermal Gradients

Yash Jaiman[1] and Prabhakar Sathujoda[2]

[1,2] Bennett University, Greater Noida UP 201310, India
yash.jaiman24@outlook.com
prabhakar.sathujoda@bennett.edu.in

Abstract. This paper deals with the thermal effects on the free vibration of a Functionally Graded (FG) porous rotor shaft system. Material properties of the FG porous rotor are temperature and position-dependent they are diversified along the radial direction of the porous FG shaft by various governing gradation laws such as power law, exponential law, and sigmoidal law, etc. The governing equations are formulated for the even porosity model in which gradation in the pore's density is defined for the even model. During the manufacturing of FGMs, various defects such as porosity can inherit in the material and degrade the quality of the fabricated part which can be catastrophically bad in high-speed rotating machinery. Sometimes a limited amount of porosity can be a good thing for instance a gradual increase in the pore imparts many properties such as mechanical shock resistance, thermal insulation, catalytic efficiency, and the relaxation of thermal stress. A modified homogenization material rule is used to describe material properties and are approximated for the FG porous rotor for different porosity phases. The material selection for which the analysis has been carried out in the case of FG porous shaft is Stainless Steel-ZrO_2. Python code has been developed for different porosity models to generate ANSYS macros to input the properties of the constituent material. The effects of porosity models, volume fraction of porosity, power law index, and temperature gradient on the vibration characteristics of a porous FG rotor bearing system are studied.

Keywords: Finite element method, porosity, functionally graded material, NLTD, temperature gradient.

1 Introduction

Functionally graded materials are a class of advanced engineering materials that are used extensively by various industries as a structural component due to their high material performance under high-temperature environments and for having high bending-stretching coupling effect. These are inhomogeneous composites that constitute gradual material transition from one material into another. The inspiration of FGMs comes from nature, various biological systems such as the trunk of trees, bones, shells, animal tissue all are highly adapted to their environment and have somewhat gradation of properties.

The most familiar FGM is composed of ceramic and metal. These materials are aggressively used by engineers and scientists as a replacement of traditional composites in various industries such as aerospace, medical, energy, automobile, high-speed transport, optoelectronics, etc. FGMs are fabricated by various manufacturing techniques according to their applications to get tailored morphologies and spatial gradation properties. Mostly these are constructive or transport-based processes which include powder deposition, liquid phase deposition, plasma spray forming, interdiffusion, macrosegregation, and segregative darcian flow processes, etc. While fabricating the FGMs, microstructure defects occur such as porosity, residual stresses, however, these defects degrade the material properties. While fabricating the FG material, microvoids and holes are formed in the FG shaft. Porosity found in some systems plays an important role in giving the material mechanical shock resistance, catalytic efficiency, thermal insulation, and relaxation of thermal stresses after certain porosity ratio materials start to lose their mechanical as well as structural strength. Thermomechanical characteristics and material properties of graded materials are very important factors in designing rotating machinery.

Based on the literature, extensive research has been done on vibration analysis of various FG structures. In 1987, Koizumi [1] ideated the concept of Functionally Graded Materials to improve the temperature resistance of structural components under high-temperature gradients for various space and aerospace applications. Nelson et al. [2] contributed to the theoretical analysis of rotating shafts that integrates the effect of gyroscopic, rotary inertia moment, and shear deformation into the Finite element (FE) shaft model. Ruhl and Booker [3] considered the effects of inertia and damping of a rotor system for which a FEM model is devised. The hysteretic and viscous damping of rotor shafts was investigated by Dimentberg [4] which show that viscous damping after first critical speeds is destabilizing and hysteretic damping at all critical speeds is destabilizing. Suresh and Mortensen [5] present an impressive introduction to the basics of FGM. Aboudi et al. [6] developed a more general higher-order theory for FG materials and demonstrated the utility of FG microstructures in tailoring structural component behaviors in different applications. Wattanasakulpong and Ungbhakorn [7] studied the dynamic behavior of porous functionally graded beams. Jahwari and Naguib [8] examined FG porous plates with various theories of plate and pattern of cellular distribution. Atmane et al. [9] investigated the dynamics of porous FG beams with different theories of beams. Ebrahimi and Jafari [10] examine the vibration properties of FG beams with porosity effect and different thermal loadings. Yang et al. [11] present a post-buckling thermo-mechanical study of cylindrical panels made of functionally graded materials (FGMs) with temperature-dependent thermo-elastic properties.

A substantial number of studies has been conducted to explain natural frequency response of metal ceramic based FGM structures, as compared insufficient work has been done on FG rotor bearing system. Earlier, much of the work was implemented using beam elements in FG structures. The primary aim of the current work is to investigate the effects of thermal gradient on the natural frequency response of the metal-ceramic based FG shaft system, which is modeled by 3-D solid elements. Through the application of power law across the radial direction of the shaft, continuous gradation of material properties is accomplished. Temperature distribution along the cross-section of the material is governed by Non-linear Temperature Distribution (NLTD) law. For even

porosity model, the effect of the porosity volume fraction and temperature gradient on the frequency response of a FG rotor system is investigated. Whirl frequencies are determined for various rotational speeds of the rotor shaft. A novel approach is used to investigate the natural frequency of the porous FG rotor bearing system by varying parameters such as temperature gradient, porosity volume fraction, and power-law index.

2 Mathematical Formulation

Due to the lack of detailed description of the exact shapes and the microstructure distribution, the determination of the efficient material properties such as modulus of elasticity, Poisson's ratio, thermal conductivity, density, shear modulus, bulk modulus is required for FGMs. Since FGMs are heterogeneous materials, effective material properties need to be determined. Precise estimation of the material property is important for the study and design of FG structures/systems to achieve the best efficiency. The material properties are determined by assuming the material to be homogeneous as well as defining volume fraction distribution and approximating phase composition of the constituent materials. Homogenization is key to determine the effective material properties and material behaviour. Various models, viz. Voigt, Reuss, Sigmoid, Mori-Tanaka are used to compute the material properties of FGMs. The inner constituent of the FG shaft is metal-rich, and the external constituent of the FG shaft is ceramic-rich, volume fraction of these materials varies across the cross-section according to different gradation laws in which gradually volume fraction of ceramics increases as we go from inner to outer of the FG shaft. The effective material properties P unique for each layer can be expressed as in Eq. 1.

$$P=P_cV_c+P_mV_m \tag{1}$$

where P_c and P_m are the material properties of the ceramic and metal, respectively. V_c and V_m are the volume fractions of ceramic and metal respectively and are related by,

$$V_c+V_m=1 \tag{2}$$

In the current study of rotor shaft system power law gradation is employed. Thus, the effective material properties are temperature-dependent and can be represented as a nonlinear temperature function [12] as in Eq.3.

$$P(T)=P_0(P_{-1}T^{-1}+1+P_1T+P_2T^2+P_3T^3) \tag{3}$$

where P_0, P_{-1}, P_1, P_2, P_3 are the material-dependent temperature coefficients are given by Reddy et al. [13].

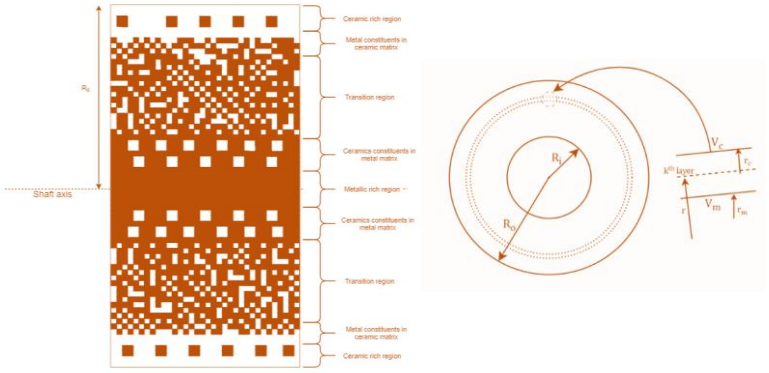

Fig. 1. (a) Cut section view of volume fraction along the radial direction throughout the FG layer (b) Cut section view of continuous gradation of the FG layer

2.1 Material properties for Porous FG Rotor Shaft in Thermo-mechanical Environment

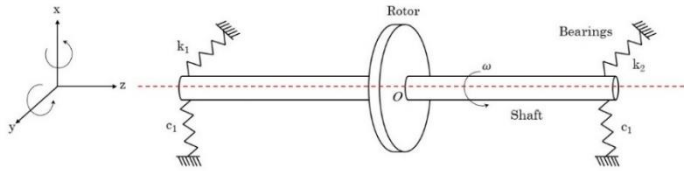

Fig. 2. Schematic diagram of a rotor shaft bearing system with the coordinate system.

Consider an FGM shaft of length L, inner radius R_i and outer radius R_o. The inner and outer constituents of the shaft are metal and ceramic, respectively. Thermo-mechanical responses of FGMs were performed by effective modeling of temperature distribution throughout the radial direction of the FG shaft. For an axisymmetric cylinder, in the absence of heat generation, temperature distribution along the radial direction of a thin circular cross-section of the FG shaft is given by the heat conduction equation.

$$\frac{d}{dr}\left[rK(r)\frac{dT}{dr} \right] = 0 \tag{4}$$

where $K(r)$ is the thermal conductivity across the radial direction of the rotor shaft. Eq.4 could be solved subjected to thermal boundary conditions as

$$\text{at } r=R_i \text{ , } T=T_m \tag{5}$$

$$\text{at } r=R_o \text{ , } T=T_c \tag{6}$$

The solution to Eq.4 could be obtained for different laws of material property gradation. Temperature distributions: Non-linear temperature distribution (NLTD) is obtained by solving the equation of heat conduction with appropriate boundary conditions shown in Eq.5 and Eq.6.

2.2 Power Law Gradation with Non-linear temperature distribution (NLTD) for Porous FG shaft

Power law is used to assign the material properties along the radial direction of the FG shaft and Non-linear temperature distribution law is used to diversify the temperature across the cross-section of the FG shaft. The volume fraction of outer (ceramic) layer in the circular FG shaft is expressed as,

$$V_o(z) = \left(\frac{r - R_i}{R_o - R_i} \right)^k \tag{7}$$

For a circular cross-section, the power law is shown in the Eq.8.

$$P(r,T) = P_m(T) + \{P_c(T) - P_m(T)\} V_o(z) \tag{8}$$

where $P(r,T)$ denotes the position and temperature-dependent properties such as Young's Modulus (E), Poisson's Ratio (v), Thermal Conductivity (K), and density (ρ). $P_m(T)$ and $P_c(T)$ temperature-dependent material properties at the metal-rich and ceramic-rich, respectively. k is the power-law index.

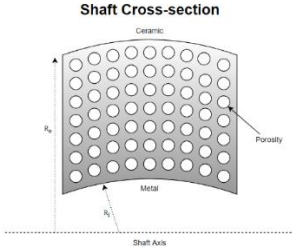

Fig. 3. Spatial distribution of porosities along the radial direction in cut-section of an FG shaft.

In the case of Porous FG shaft or cylinder, the power law is modified for even porosity model as in the Eq.9. The material properties are dependent on the volume fraction of porosity since the porosities are present in the FG shaft.

$$P(r,\alpha,T) = P_m(T) + \{P_c(T) - P_m(T)\} \left(\frac{r - R_i}{R_o - R_i} \right)^k - \{P_c(T) + P_m(T)\} \frac{\alpha}{2} \tag{9}$$

$\alpha << 1$, $R_i \le r \le R_o$, $0 \le k \le \infty$, α is the porosity volume fraction.

The solution of Eq.4 subjected boundary condition Eq.5 and Eq.6, considering seven terms of the polynomial expansion [14] gives Eq.10 as

$$T(r) = T_m + (T_c - T_m) \left[\sum_{j=0}^{5} \left\{ \frac{(-1)^j}{jk+1} \left(\frac{\kappa_{cm}}{\kappa_m} \right)^j \left(\frac{r - R_i}{R_o - R_i} \right)^k \right\} \right] \Bigg/ \left[\sum_{j=0}^{5} \left\{ \frac{(-1)^j}{jk+1} \left(\frac{\kappa_{cm}}{\kappa_m} \right)^j \right\} \right] \tag{10}$$

where $\kappa_{cm} = \kappa_c - \kappa_m$, κ_c and κ_m refers to the thermal conductivity of the ceramic rich region and the metal-rich region at a given temperature.

2.3 Modeling of material properties in current work

In the present work, the porous FG rotor shaft is composed of Stainless Steel (SUS304) and Zirconia (SS-ZrO_2) which is divided into 20 layers radially along the cross-section

of the shaft to obtain a continuous distribution of material properties. A Python code was developed to generate the ANSYS macros which distribute the material property in the spatial direction radially along the volume of the shaft. Variation of various material properties such as Young's Modulus, Poisson's Ratio, and temperature distribution profile are obtained.

In the present work, to obtain an accurate assignment of density along the cross-section of the porous FG shaft, the average density is assigned to each layer. The average density function show variation for power law.

$$\rho_{avg} = \int_{r_1}^{r_2} \left[(\rho_c - \rho_m) \left(\frac{r - R_i}{R_o - R_i} \right)^k + \rho_m \right] dr \Bigg/ \int_{r_1}^{r_2} dr \tag{11}$$

where ρ_c and ρ_m are densities of the ceramic rich and metal-rich region, respectively. r_1 and r_2 are the inner and outer radius of the selected layer. Eq.11 provides a precise uniform density distribution along the cross-section by assigning mid-radius density directly to the layer.

3 Finite Element Modelling and Analysis

A single disk rotor is rigidly mounted on a shaft which is supported by two identical isotropic bearings has been modeled and analyzed using solid elements. All dimensions of this system are given in Table 1. The shaft does not contain any internal damping effects and bearings have stiffness in both x (K_{xx}) and y (K_{yy}) directions. Effects of damping and cross-coupling are also not considered.

Table 1. Geometric dimension and Mechanical properties of FG rotor shaft system.

Parameter	Dimension
Rotor shaft length (m)	0.5
Rotor shaft radius (m)	0.01
Disk radius (m)	0.075
Disk thickness (m)	0.04
Bearing Stiffness (MN/m)	0.1
Damping Coefficient (Ns/m)	100

SOLID-185 structural element is used to model the rotor shaft and disc. The model is discretized in 20 layers along the radial direction. The disc is made of steel and the shaft is made of functionally graded material. COMBIN-14 spring-damper element is used to model the isotropic bearings. SHELL-181 shell element is used to get the layered structure of the functionally graded shaft. The natural frequency analysis of the FG rotor shaft system has been studied in two conditions. In the first case, the rotor system is stationary and in the latter case, the rotor shaft rotates at an angular speed of 5000 rpm. In the stationary reference frame, the Coriolis effect was applied to the shaft system for calculating the gyroscopic damping matrix.

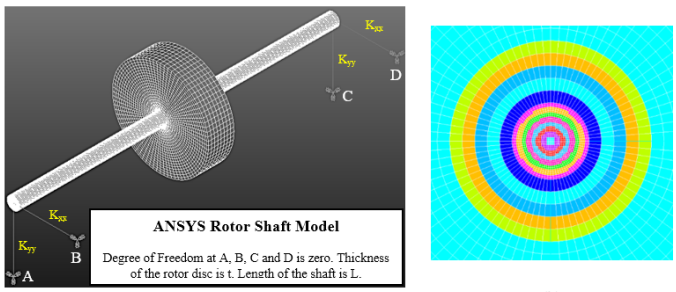

Fig. 4. (a) Single-disc rotor shaft system with bearing support in ANSYS. (b) The contour of the cross-section of each layer of the FG shaft using ANSYS model.

Table 2. Material Properties of FGM composites.

Properties	Stainless Steel (SUS-304)	Aluminum Oxide (Al_2O_3)	Zirconium Oxide (ZrO_2)	Titanium (Ti-6Al-4V)
Young's Modulus(GPa)	190	215	171.03	120
Density(kg/m^3)	7850	3980	5700	4420
Poisson's Ratio	0.265	0.21	0.24	0.31

4 Solution Procedure and System Equations

The governing equation of the complete rotor-bearing system can be expressed as

$$[M]\{\ddot{q}\} - \Omega[G]\{\dot{q}\} + [K]\{q\} = f(t) \tag{12}$$

Where $[M]$ is the global mass matrix including the rotary and translational masses of the shaft as well as the disc, $[G]$ is the global gyroscopic matrix, $[K]$ is the global stiffness matrix including the stiffness of the shaft and bearings. $\{q\}$ is the global nodal displacement vector, Ω is the rotor spin speed and $f(t)$ is the global external force vector. Assuming that for the free vibration analysis, external forces and gravity forces are neglected. QR Damped eigenvalue method is applied to find out the natural frequency and whirl frequencies of the FG rotor shaft system. For the solution, the coordinate transformation was used to transform the eigenvalue problem to modal subspace [15]

$$\{q\} = [\Psi]\{\Phi\} \tag{13}$$

where $[\Psi]$ is normalized eigenvector matrix for the mass matrix $[M]$, $\{\Phi\}$ is the modal coordinate matrix. Using transformation for the differential equation of motion in modal subspace [16] can be written as

$$[I]\{\ddot{\Phi}\} + [\Psi]^T[C][\Psi]\{\dot{\Phi}\} + \left([\Lambda^2] + [\Psi]^T[K_{unsym}][\Psi]\right)\{\Phi\} = 0 \tag{14}$$

where [I] is the inertia matrix, [C] is a non-singular damping matrix, and [Λ^2] is a diagonal matrix containing the first n eigenfrequencies ω.

5 Validations

A finite element model has been developed in ANSYS to compute natural and whirl frequencies of a porous FG Jeffcott rotor system. A step-by-step validation of power-law, NLTD, finite element model and natural frequencies was carried out and presented in the following subsections.

5.1 Code Validation

A Python code has been generated to distribute the material property in the spatial direction radially along the volume of the shaft. The plot of Young's Modulus for various power-law coefficients is shown in Figure 6. The inner core temperature of the shaft is kept at 300K and the outer ceramic at 900K. The distribution profiles are in absolute agreement with the graphs present in the literature. The plot of Poisson's Ratio vs radial distance for various power-law coefficients is shown in Figure 7.

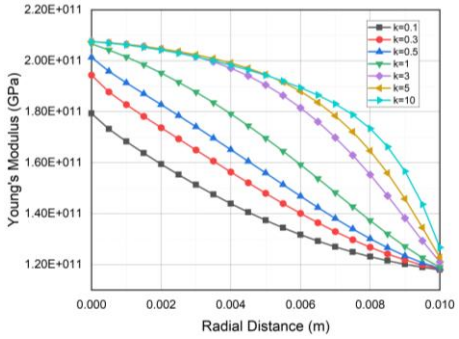

Fig. 5. Radial variation of Young's Modulus for different k values when T_m=300K and T_m=900K for SS-ZrO_2.

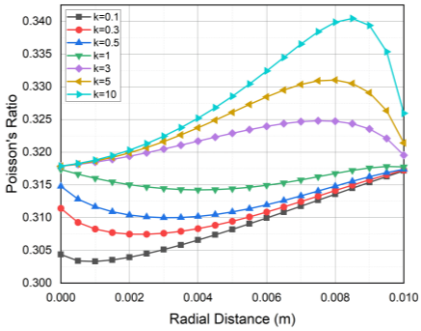

Fig. 6. Radial variation of Poisson's Ratio for different k values when T_m=300K and T_m=900K for SS-ZrO_2.

5.2 Temperature distribution using NLTD

The radial variation of temperature achieved using NLTD for an FG shaft. The graphs obtained are the desired representation of exponential nature. The plots confirm that the temperature distribution along the radial direction is governed by power-law and varies temperature according to the law. This temperature variation depends on various parameters such as thermal conductivity, Young's Modulus, density which is a function of the radius of the shaft.

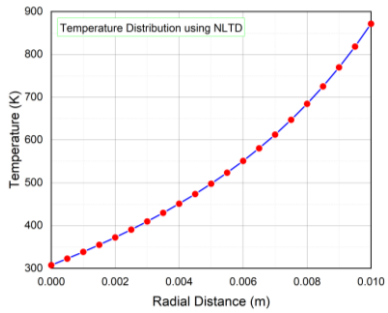

Fig. 7. Temperature distribution using NLTD in SS-ZrO_2 FG shaft.

5.3 Verification of developed equations for porous FG shaft

For even porosity model equations are developed and are radially distributed along the cross-section. In the case of SS-ZrO_2, the variation of densities for each layer according to the equations developed for each model and the rate of variation can be seen in Fig. 8.

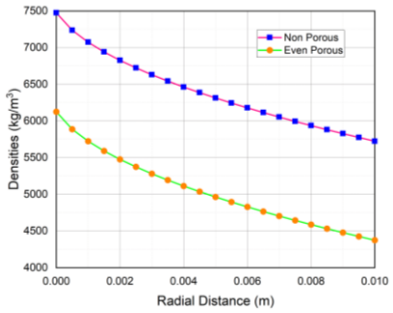

Fig. 8. Density variation plots for even porosity model in case of SS-ZrO_2 FG shaft at room temperature.

5.4 Validations for Non-dimensional Natural frequencies for Porous FG Beam

Due to inadequate research on porous FG shaft. For validation of porosity modeling, we have used a porous FG beam with a rectangular cross-section. The FG beam consists of Titanium and Zirconia Oxide at the top and bottom surface, respectively. The FG beam has not been subjected to any temperature gradient. FG beam is considered at

room temperature. The dimensions of the FG beam are taken from ref.[14]. The slenderness ratio (L/h) of the beam is kept as constant i.e., equal to 20. The FG beam is simply supported. Non-dimensional frequencies of the FG beam are obtained by Eq.15.

$$\bar{\omega} = \omega \frac{L^2}{h} \sqrt{\frac{\rho_m}{E_m}} \tag{15}$$

where ω is the natural frequency of the FG beam and E_m is the Young's Modulus. The frequencies show significant similarity with the works of Ebrahimi et al.[14] as tabulated in the Table 3.

Table 3. Non-dimensional natural frequencies for Porous FG beam (Ti-ZrO_2).

α	k=0.5			k=2		
	Ebrahimi et al.[14]	Current	% error	Ebrahimi et al.[14]	Current	% error
0	4.515	4.518	0.066	3.55	3.561	0.309
0.1	4.582	4.584	0.043	3.508	3.513	1.423
0.2	4.667	4.671	0.085	3.449	3.453	0.115

6 Results and Discussion

A single-disc FG rotor bearing system composed of SS-ZrO_2 is considered to study the natural frequencies and whirl frequencies. Three-dimensional finite element modeling has been carried out for power law.

6.1 Effect of temperature gradient and porosity volume fraction on natural frequencies

The fundamental frequencies of the functionally graded porous shaft are calculated and presented in the figures for different volume fractions of porosity, porosity models, temperature gradients, and power law indices. In the study, the initial temperature gradient is considered as $\Delta T = 0$ (K). The eigenfrequencies of the porous rotor shaft at stationary conditions are decreasing with increase in the power-law index. Power-law coefficients are varied from 0.1 to 10 to evaluate the effect of eigenfrequencies on the thermal gradient of the FG rotor bearing system from 0 to 600K. From Figure 10, It is observed that there is a decrease in eigenfrequency. As can be noted from the graph the eigenvalue difference is much larger for smaller values of the power-law index as compared to larger values of the power-law indices where values do not vary as much. With the increase in temperature gradient of the system, eigenfrequencies decrease, and this can be attributed to the stiffness of the system.

For different porosity volume fraction, the variation of natural frequency for various power-law indexes. Different trends have been recorded in Figure 11. The figure depicts that frequency variation is much steep for lower power law indices as compared to a higher power law index. The reasoning behind this variation can be attributed to Young's Modulus and the mass of the rotor shafts.

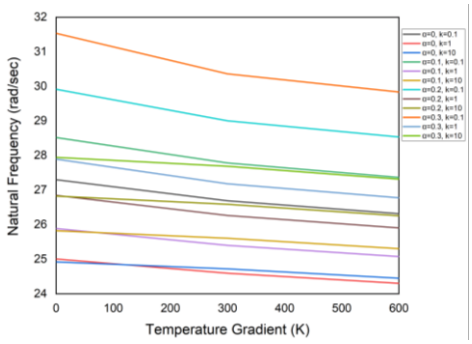

Fig. 9. Natural frequency variation for FG shaft under thermal gradient for different cases.

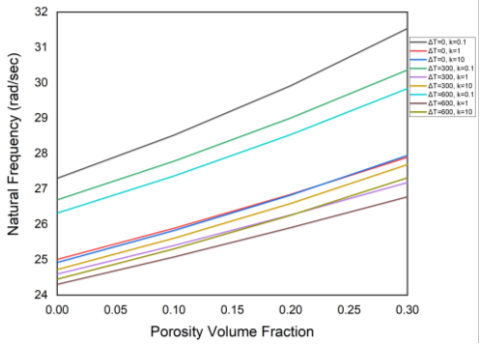

Fig. 10. Natural frequency variation with porosity parameter(α) for different cases.

6.2 Effect of temperature gradient and porosity volume fraction on whirl frequencies

The effects of thermal gradient and porosity on whirl frequencies for porous FG rotor shaft of SS-ZrO_2 shown in Figure 4(a). In the current section, results have been presented for different thermal gradient and porosity cases. The temperature has been varied for different outer ceramic temperature (T_c) and keeping the inner metallic (T_m) temperature constant. The shaft has been exposed to three different thermal gradients with different outer ceramic temperature (T_c) and constant inner metallic temperature (T_m) constant. For each thermal gradient case, seven power-law indexes are varied from 0.1 to 10 to account for the whirl effects on a thermal gradient. Whirl frequencies are varied for different thermal gradient, porosity volume fraction, and power-law index. Trends generated in the frequency variation has been represented graphically in figures. Due to gyroscopic effects, the frequency pairs splits into two at higher rotational speed namely Forward Whirl(FW) and Backward Whirl(BW). Comparative studies of the variation of whirl frequencies for porous FG rotor shaft has been carried out for different cases shows Campbell diagram of porous FG shaft considering with and without porosity for different thermal gradients. For the FG rotor system, the first two FW and BW are analyzed for the rotating speed of the shaft at 5000rpm concerning the various temperature gradient and porosity volume fraction. The trends show that the whirl frequency value decreases as the temperature gradient increases. A key observation from

the Campbell diagram is that splitting of the FW and BW occurs more as we increase the temperature gradient and a higher value of porosity volume fraction of the rotor shaft.

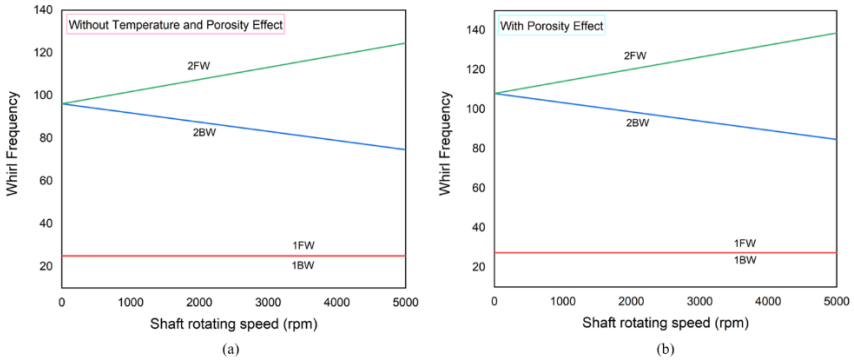

Fig. 11. Campbell diagram for (a)ΔT=0, α=0, k=1 (b) ΔT=0, α=0.2, k=0.5.

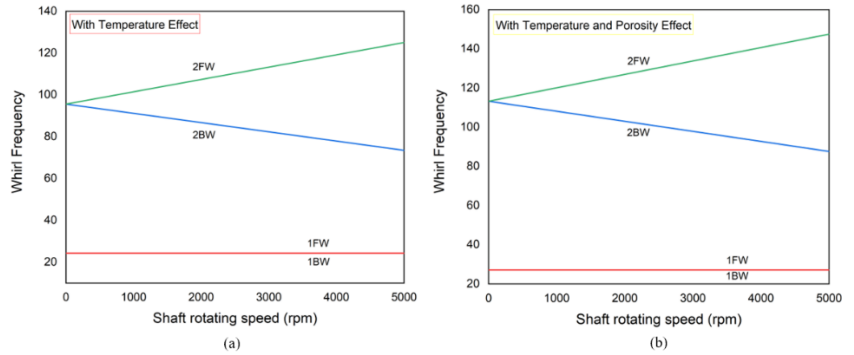

Fig. 12. Campbell diagram for (a)ΔT=600, α=0, k=1 (b) ΔT=600, α=0.3, k=0.5.

7 Conclusions

In the current investigation, a 3-D FEM technique was carried out in commercial ANSYS software. The shaft constitutes an SS-ZrO_2 combination in a continuous gradation fashion as governed by a power law. The rotor shaft is held on isotropic bearings from both sides. For designing and analyzing the FG rotor shaft, solid elements are used. The rotor shaft is subjected to various temperature gradients and different porosity parameters. Main findings rely on the vibration study of a porous functionally graded shaft employing Python code script. The three-dimensional Finite Element Method is used for designing and natural frequency study of functionally graded rotor system in a thermo-mechanical environment. By varying different temperature gradients and power-law indexes, the spatial distribution of material properties was radially obtained. Natural frequency is obtained for various temperature gradient and power-law index and observed that the natural frequency reduces as temperature increases. The effect of porosity on an FG shaft in a thermal condition is studied and found that the natural frequency decreases with an increase in both the porosity and temperature. Whirl

effects are analyzed for various conditions with or without temperature gradient and porosity volume fraction and observed that the splitting of whirl pairs increases as the temperature and porosity increase. Finally, it can be concluded that the current work can be used for modeling and frequency analysis of an FG rotor shaft system in a thermal environment.

References

1. Koizumi, M., 1993, "Concept of FGM," *Ceramic Trans.*, 34, pp. 3–10.
2. Nelson, H.D., Mcvaugh, J.M., 1976, "The dynamics of rotor-bearing systems using finite element method," *Journal of Engineering for Industry*, 98, pp. 593–600.
3. Ruhl R, Booker JF, A finite element model for distributed parameter turbo rotor systems. J Eng Ind 1972; 94: 128-132.
4. Dimentberg FM, Flexural vibrations of rotating shafts. London: Butterworths, 1961
5. Suresh, S., Mortensen, A., 1998, "Fundamentals of functionally graded materials", London, UK: IOM Communications Limited.
6. Aboudi, J., Pindera, M.J., Arnold, S.M., 1999, "Higher-order theory for functionally graded materials," *Composites, Part B: Engineering*, 30 (8), pp.777–832.
7. Wattanasakulpong, N. and Ungbhakorn, V. [2014] "Linear and nonlinear vibration analysis of elastically r estrained ends FGM beams with porosities," *Aerospace Science and Technology* 32(1), 111–120.
8. Jahwari, F. and Naguib, H. E. [2016] "Analysis and homogenization of functionally graded viscoelastic porous structures with a higher order plate theory and statistical based model of cellular distribution," *Applied Mathematical Modelling* 40(3), 2190–2205.
9. Atmane, H. A., Tounsi, A., Bernard, F. and Mahmoud, S. R. [2015] "A computational shear displacement model for vibrational analysis of functionally graded beams with porosities," *Steel and Composite Structures* 19(2), 369–384.
10. Ebrahimi, F. and Jafari, A. [2016] "A higher-order thermomechanical vibration analysis of temperature-dependent FGM beams with porosities," *Journal of Engineering* 2016, 20pp., doi:10.1155/2016/9561504.
11. Yang, J., Liew, K., Wu, Y. and Kitipornchai, S., 2006. Thermo-mechanical post-buckling of FGM cylindrical panels with temperature-dependent properties. *International Journal of Solids and Structures*, 43(2), pp.307-324.
12. Touloukian, Y. S. [1967] Thermophysical Properties of High Temperature Solid Materials (Macmillan, New York).
13. Reddy, J. N. and Chin, C. D. [1998] "Thermoelastical analysis of functionally graded cylinders and plates," *Journal of Thermal Stresses* 21(6), 593–626.
14. Kiani Y, Eslami MR. Thermal buckling analysis of functionally graded material beams. *Int J Mech Mater Des* 2010;6(3):229–38.
15. ANSYS Theory Manual